

Final-State Interaction in Electron Scattering by Polarized Nuclei¹

J.E. Amaro^a and T.W. Donnelly^b

^a *Departamento de Física Moderna, Universidad de Granada, Granada 18071, Spain*

^b *Center for Theoretical Physics, Laboratory for Nuclear Science and Dept. of Physics,
Massachusetts Institute of Technology, Cambridge, MA 02139, U.S.A.*

Abstract

The cross section for the reaction ${}^{39}\vec{\text{K}}(e, e'p){}^{38}\text{Ar}$ is computed, and the dependence of the FSI on the initial polarization angles of the nucleus ${}^{39}\text{K}$ is analyzed. The results are explained in a semi-classical picture of the reaction. This procedure allows us to find the best initial kinematical conditions for minimizing the FSI.

1 Introduction

In this talk we explore the effects of the FSI in $(e, e'p)$ reactions using polarized nuclei. All of the measurements to date involving medium and heavy nuclei have been performed with unpolarized targets [1] and hence only the global effects of FSI averaged over all polarization directions have been addressed experimentally. Using instead polarized nuclei as targets, new possibilities to extract the full tri-dimensional momentum distribution of nuclei will become available [2, 3, 4, 5].

The few theoretical studies of $(e, e'p)$ reactions involving polarized, medium and heavy nuclei in DWIA [6, 4, 7, 8] report a dependence of FSI effects — or nuclear transparency — on the choice of polarization angles. In the present work we show that these variations of the transparency can be understood in terms of the orientation of the initial-state nucleon's orbit and of the attenuation of the ejected nucleon's flux.

We shall show that one is able to predict the orientations of the target polarization that are optimal for minimizing the FSI effects, providing the ideal situations for nuclear structure studies. This situation occurs when the nucleon is ejected directly away from the nuclear surface. On the other hand, when the nucleon is ejected from the nuclear surface but in the opposite direction — into the nucleus — it has to cross the entire nucleus to exit on the opposite side, and the FSI effects are then found to be maximal. This second situation is ideal for detailed studies of the absorptive part of the FSI. All of these situations can be selected simply by changing the direction of the nuclear polarization.

¹Talk presented by J.E. Amaro at the IVth Workshop on Electromagnetically induced Two-Hadron Emission, Granada, Spain, 1999

2 Coincidence cross section of polarized nuclei. Results

Here we present the results of a DWIA calculation of the $^{39}\vec{K}(e, e'p)^{38}\text{Ar}_{g.s.}$ cross section in the extreme shell model. The present choice is prototypical and the results can be generalized for any polarized nucleus and can be addressed using more sophisticated nuclear models.

We describe the ground state of $^{39}\vec{K}$ as a hole in the $d_{3/2}$ shell of ^{40}Ca . The initial nuclear state is 100% polarized in the direction $\Omega^* = (\theta^*, \phi^*)$.

$$|A(\Omega^*)\rangle = R(\Omega^*)|d_{3/2}^{-1}, m = \frac{3}{2}\rangle, \quad (1)$$

where $R(\Omega^*)$ is a rotation operator. In this simple model the nuclear polarization is carried by the hole in the $d_{3/2}$ shell. The polarization angles (θ^*, ϕ^*) are the spherical coordinates of the polarization vector Ω^* with respect to the \mathbf{q} -direction (z -axis) and with the x -axis in the scattering plane.

The final hadronic state is given by a proton in the continuum with energy ϵ' and momentum \mathbf{p}' , plus a daughter $A - 1$ nucleus (^{38}Ar) in the ground state. This is described in the shell model as two holes in the $d_{3/2}$ shell coupled to total spin $J = 0$.

The hole wave function is obtained by solving the Schrödinger equation with a Woods-Saxon potential. The wave function of the ejected proton is obtained by solving the Schrödinger equation with an optical potential for positive energies.

We compute the cross section as

$$\Sigma \equiv \frac{d\sigma}{dE'_e d\Omega'_e d\Omega'} = \sigma_M (v_L \mathcal{R}^L + v_T \mathcal{R}^T + v_{TL} \mathcal{R}^{TL} + v_{TT} \mathcal{R}^{TT}), \quad (2)$$

where σ_M is the Mott cross section, v_K are the electron kinematical factors given in [9], and \mathcal{R}^K are the nuclear response functions. See Refs. [7, 8] for more details of the model.

Next we show results of a calculation of the $(e, e'p)$ cross section for different nuclear polarizations (θ^*, ϕ^*) . The kinematics correspond to the quasi-elastic peak and in-plane emission

$$q = 500 \text{ MeV}/c, \quad \omega = 133.5 \text{ MeV}, \quad \phi = 0, \quad \theta_e = 30^\circ$$

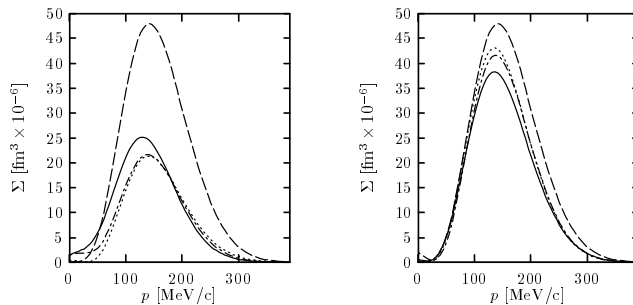


Figure 1: Cross section computed for two values of the nuclear polarization angles. Left: $\theta^* = 90^\circ$, $\phi^* = -90^\circ$; right: $\theta^* = 90^\circ$, $\phi^* = 90^\circ$. The meaning of the curves is the following: solid: DWIA; dashed: PWIA; dotted: DWIA but with just the imaginary part of the central optical potential; dash-dotted: DWIA without spin-orbit contributions.

In fig. 1 we show the cross section for $^{39}\vec{\text{K}}$ polarized in the $-y$ direction, (left) and in the y direction (right). The solid lines are the full DWIA calculation, using the optical potential of Schandt et al. The dashed lines are the cross sections computed in PWIA, i.e., without FSI. The dotted lines correspond to the DWIA, but including in the FSI just the central imaginary part of the optical potential, while the dash-dotted lines include in addition the central real part of the potential.

Comparing the solid and dashed lines, we see that the effect of the FSI (solid lines relative to dashed lines) is quite dependent on the polarization of the nucleus. This fact suggest that the “transparency” of the nucleus to proton propagation can be maximized or minimized by selecting a particular polarization of the nucleus and that if one is able to understand physically the different behavior seen for the FSI effects in fig. 1, then it could be possible to make specific predictions about the reaction for future experiments.

3 A semi-classical picture of the reaction

In order to understand physically the above results we will consider a semi-classical model of the reaction by assuming it to take place in two or more steps as follows: first a proton with (missing) momentum \mathbf{p} and energy ϵ is knocked-out by the virtual photon and it acquires momentum \mathbf{p}' and energy $\epsilon' = \epsilon + \omega$. Second, as this high-energy nucleon traverses the nucleus it undergoes elastic and inelastic scattering which, in our model, are produced by the real and imaginary parts of the optical potential.

The important point here is that the nucleus is polarized in a specific direction. Accordingly, the initial-state nucleon can be localized in an oriented (quantum) orbit. From the knowledge of this orbit and of the missing momentum one can predict the most probable location of the struck proton, and therefore one can specify the quantity of nuclear matter that the proton must cross before exiting from the nucleus with momentum \mathbf{p}' .

We illustrate the case of a particle in a $d_{3/2}$ wave. which is the relevant state for our calculation. First consider that the particle is polarized in the z -direction ($\mathbf{\Omega}^* = \mathbf{e}_3$). The corresponding wave function can be written as

$$|\frac{3}{2}\frac{3}{2}\rangle = \psi_1|\uparrow\rangle + \psi_2|\downarrow\rangle. \quad (3)$$

where the up and down components are given by

$$\psi_1 = -\sqrt{\frac{3}{8\pi}} \sin\theta \cos\theta e^{i\phi} R(r) \quad (4)$$

$$\psi_2 = -\sqrt{\frac{3}{8\pi}} \sin^2\theta e^{2i\phi} R(r). \quad (5)$$

Here the angles (θ, ϕ) are the spherical coordinates of the particle’s position \mathbf{r} and $R(r)$ is its radial wave function. The spatial distribution is then given by the single-particle probability density

$$\rho(\mathbf{r}) = |\psi_1|^2 + |\psi_2|^2 = \frac{3}{8\pi} \sin^2\theta |R(r)|^2. \quad (6)$$

Taking into account the form of the radial wave function for the $d_{3/2}$ wave, we can see that the particle is distributed around the center of the nucleus in a toroidal-like (quantum) orbit as shown schematically in fig. 2 (upper part). In a semi-classical picture of the bound state, we can imagine the particle performing a rotatory orbit within the torus in a counter-clock sense, as shown in the figure. The shape of the distribution for arbitrary polarization $\mathbf{\Omega}^*$ is just a rotation of the above distribution, as also shown in fig. 2 (bottom).

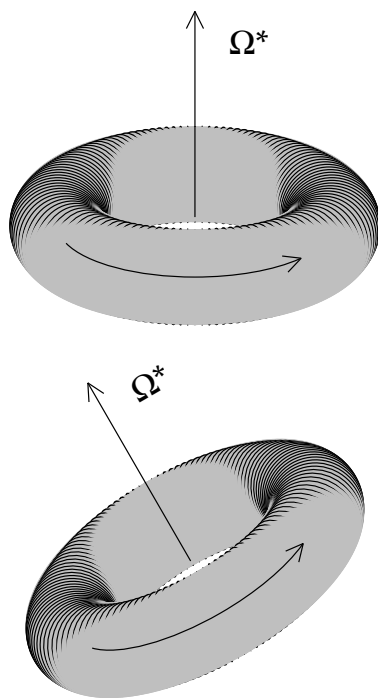


Figure 2: Pictorial representation of the spatial distribution of a proton in the $d_{3/2}$ shell, shown as a torus-like distribution for two different polarizations.

The next step is to localize the particle within the orbit for a given value of the missing momentum \mathbf{p} . From elementary quantum mechanics we employ the Fourier transform $\tilde{\psi}(\mathbf{p})$ of the wave function and the position operator in momentum space $\hat{\mathbf{r}} = i\nabla_p$ to define the local position of the nucleon in the orbit for momentum \mathbf{p} in the following way:

$$\mathbf{r}(\mathbf{p}) = \frac{\text{Re } \tilde{\psi}^\dagger(\mathbf{p})(i\nabla_p)\tilde{\psi}(\mathbf{p})}{\tilde{\psi}^\dagger(\mathbf{p})\tilde{\psi}(\mathbf{p})}. \quad (7)$$

This is a well-defined vector which represents the most probable location of a particle with momentum \mathbf{p} when it is described by a wave function ψ . Henceforth $\mathbf{r}(\mathbf{p})$ represents the position of the particle in the orbit in the present semi-classical model.

For the case of interest here of the $d_{3/2}$ orbit polarized in the z -direction, we compute the position $\mathbf{r}(\mathbf{p})$ by using the wave function given in eqs. (3–5) in momentum space:

$$\text{Re } \tilde{\psi}^\dagger(\mathbf{p})i\nabla_p\tilde{\psi}(\mathbf{p}) = -\frac{3}{8\pi} \frac{|\tilde{R}(p)|^2}{p} \sin\theta(1 + \sin^2\theta)\hat{\phi}, \quad (8)$$

where now (θ, ϕ) are the spherical coordinates of the missing momentum \mathbf{p} , $\tilde{R}(p)$ is the radial wave function in momentum space, and $\hat{\phi}$ is the unit vector in the azimuthal direction. As we see, upon dividing by the momentum distribution (given by eq. (6), but in momentum space)

$$\tilde{\psi}^\dagger(\mathbf{p})\tilde{\psi}(\mathbf{p}) = \frac{3}{8\pi} \sin^2\theta|\tilde{R}(p)|^2, \quad (9)$$

the radial dependence in the numerator and denominator goes away, and we obtain an expectation value of position which is independent of the radial wave function

$$\mathbf{r}(\mathbf{p}) = -\frac{1 + \sin^2\theta}{p \sin\theta} \hat{\phi}. \quad (10)$$

This expression has been obtained for the polarization in the z -direction. For a general polarization vector $\boldsymbol{\Omega}^*$ we just perform a rotation of the vector $\mathbf{r}(\mathbf{p})$. Introducing the angle θ_p^* between \mathbf{p} and $\boldsymbol{\Omega}^*$, we can write the nucleon position in a general way

$$\mathbf{r}(\mathbf{p}) = -\frac{1 + \sin^2\theta_p^*}{p^2 \sin^2\theta_p^*} \boldsymbol{\Omega}^* \times \mathbf{p}. \quad (11)$$

Using the above definitions we can give a physical interpretation of the results shown in fig. 1. The kinematics for the case of the ^{39}K nucleus polarized in the $-y$ direction are illustrated in fig. 3(a). Therein, the momentum transfer points in the z -direction and we show the missing-momentum vector \mathbf{p} corresponding to the maximum of the momentum distribution, $p \sim 140$ MeV/ c . The momentum of the ejected proton \mathbf{p}' is also shown in the picture. For $\boldsymbol{\Omega}^*$ pointing in the $-y$ direction, the semi-classical orbit lies in the xz -plane and follows a counter-clockwise direction of rotation. For these conditions, the most probable position of the proton before the interaction is indicated with a black dot near the bottom of the orbit. As the particle is going up with momentum \mathbf{p}' after the interaction with the virtual photon, it has to cross all of the nucleus and exit it by the opposite side; thus one expects that the FSI will be large in this situation, as shown in the left panel of fig. 1.

In fig. 3(b) we show the picture for the opposite polarization in the y -direction. In this case the nucleon distribution in the orbit is the same as in (a), but the rotation direction is the opposite, Hence now it is more probable for the nucleon to be located near the upper part of the orbit. As the nucleon is still going up with the same momentum \mathbf{p}' , the distance that it has to travel through the nucleus is

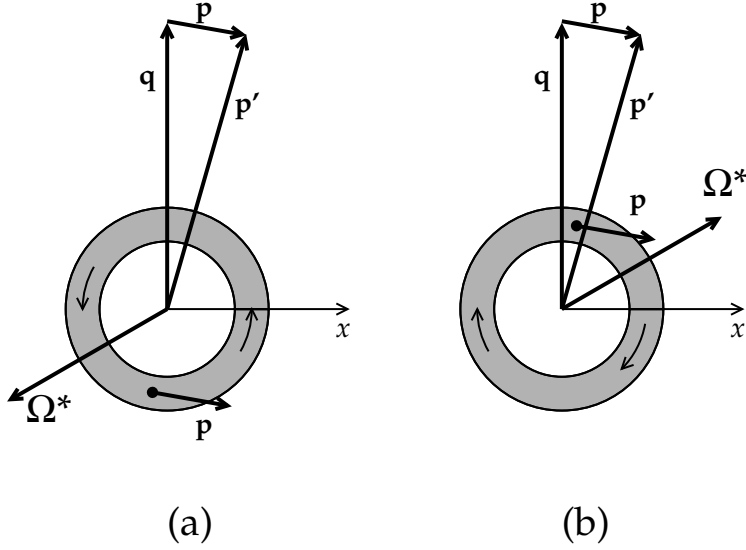


Figure 3: Semi-classical orbit and location of the proton for the same kinematics and nuclear polarizations as in Fig. 1.

much smaller than in case (a), and hence one expects small FSI effects, namely, what is seen in the right panel of fig. 1.

We have arrived at a very intuitive physical picture of why the FSI effects differ for different orientations of the nuclear spin: the polarization direction fixes the orientation of the nucleon distribution (quantum orbit). For a given value of the missing momentum one can locate the particle in a definite position within the orbit, and therefore within the nucleus. Assuming that the particle leaves the nucleus with the known momentum \mathbf{p}' , one can determine the quantity of nuclear matter that it has to cross before exiting.

In order to check the above picture for any nuclear polarization, we have computed the cross section for a set of 26 different nuclear polarization angles expanding the (θ^*, ϕ^*) plane. Using equation (11) we have computed the distance s of the nucleon trajectory within the nucleus, by choosing some appropriate value for the nuclear radius R . A model of exponential attenuation of the cross section due to nuclear absorption can be crafted in the following way:

$$\Sigma_{DWIA} \simeq \Sigma_{PWIA} e^{-s/\lambda}, \quad (12)$$

where λ is a free parameter to be interpreted as the mean free path (MFP). Within this approximation, the nuclear transparency, defined as the ratio between the DWIA and PWIA results, can be written as

$$T \equiv \frac{\Sigma_{DWIA}}{\Sigma_{PWIA}} \simeq e^{-s/\lambda}. \quad (13)$$

In fig. 4 we show the nuclear transparency as a function of the distance s to the nuclear surface, computed for different polarizations, at the maximum of the cross section. For the FSI we have used just the central, imaginary part of the optical potential. In this figure we see that the dependence of $\log T$ can in fact be approximated by a straight line. By performing a linear regression we obtain a MFP of $\lambda = 8.4$ fm. This value is quite independent of the radius R in the region between $r_{1/2}$ and $r_{1/10}$, where the nuclear density $\rho(r)$ takes the values $\rho(0)/2$ and $\rho(0)/10$, respectively.

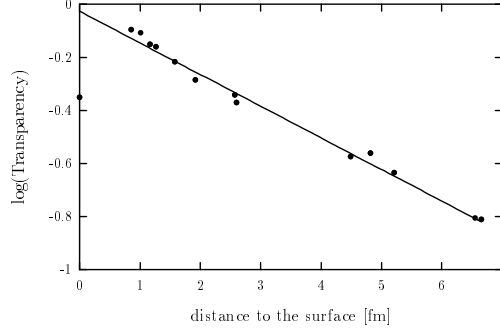


Figure 4: Nuclear transparency as a function of the nucleon path s within the nucleus for different nuclear polarizations. The FSI only include the imaginary part of the central optical potential.

4 Applications to two-particle emission reactions

Finally we give a possible application of the above model to two-hadron emission reactions. Consider $(e, e'N\pi)$ reactions from polarized nuclei in the Δ -region. By selecting the appropriate nuclear polarization, one could reduce or enhance the FSI of the final Δ in the nuclear medium. In fact, using the above model, one has control on the point of the nucleus where the Δ is created. Making a crude estimation of the length that the Δ travels before decaying

$$x \sim \frac{\hbar c}{\Gamma_{\Delta}} \sim \frac{200}{120} \text{ fm} \sim 1.7 \text{ fm} \quad (14)$$

we see that it could be possible to produce the Δ in the two situations shown in figure 5. In the case (a)

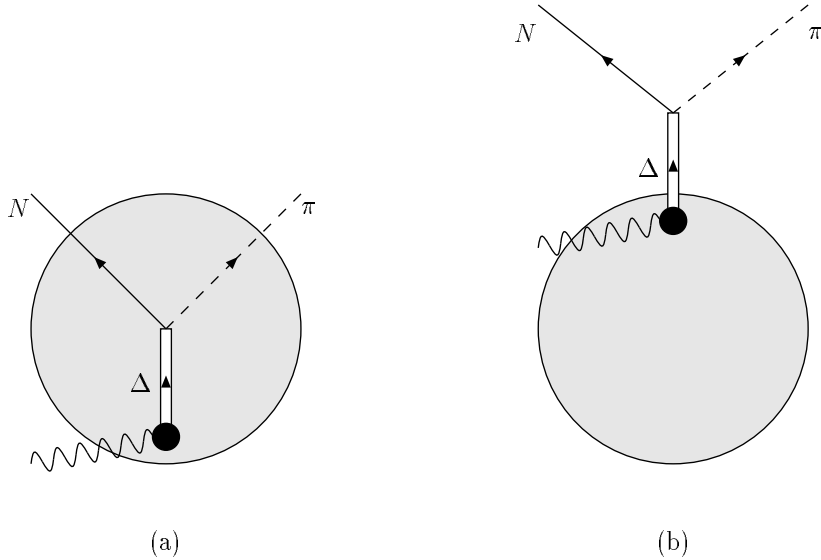


Figure 5: Electroproduction of a Δ from a polarized nucleus for two different nuclear polarization directions.

the Δ is created near the nuclear surface and propagates into the nucleus. It has large FSI and decays

inside the nucleus into a pair $N + \pi$ which also interacts with the nucleus. In the second case (b) the Δ propagates out of the nucleus. The FSI of the Δ is expected to be smaller. The Δ decays outside of the nucleus. This situation is cleaner to study the Δ electroproduction amplitude in nuclei without too much distortion by FSI. Case (a) is ideal to study the Δ properties in the nuclear medium.

5 Summary and conclusions

We have studied the reaction $^{39}\text{K}(e, e'p)^{38}\text{Ar}_{\text{gs}}$ for polarized ^{39}K in DWIA. We have studied the dependence of the FSI as a function of the nuclear polarization direction and introduced a physical picture of the results in order to understand the different effects seen in the cross section.

The argument to explain the FSI effects is based on the PWIA and it has been illustrated by introducing the semi-classical concept of a nucleon orbit within the nucleus. For given kinematics we can fix the expectation value of the position of the nucleon within the nucleus before the interaction. From this information we have computed the length of the path that the nucleon travels across the nucleus for each polarization.

Our results show that when the FSI effects are large the computed nucleon path through the nucleus is also large, whereas the opposite happens when the FSI effects are small. Thus, by selecting the appropriate nuclear polarization, one can reduce or enhance the FSI effects. Such control should prove to be very useful in analyzing the results from future experiments with polarized nuclei.

Finally, our model can also be applied to the $(e, e'N\pi)$ reaction in the Δ peak. Since by flipping the nuclear polarization one can go from big to small FSI effects of the Δ , this opens the possibility of using this kind of reaction to distinguish the FSI effects from other issues of interest, such as the Δ electroproduction amplitudes in the medium.

Acknowledgments

This work is supported in part by funds provided by the U.S. Department of Energy (D.O.E.) under cooperative agreement #DE-FC01-94ER40818, in part by DGICYT (Spain) under Contract No. PB92-0927 and the Junta de Andalucía (Spain) and in part by NATO Collaborative Research Grant #940183.

References

- [1] S. Boffi, C. Giusti, F. D. Pacati and M Radici, *Electromagnetic Response of Atomic Nuclei*, Oxford University Press, 1996
- [2] J.A. Caballero, T.W. Donnelly and G.I. Poulis, *Nucl. Phys.* **A555** (1993) 709.
- [3] J.A. Caballero, T.W. Donnelly, G.I. Poulis, E. Garrido and E. Moya de Guerra, *Nucl. Phys.* **A577** (1994) 528.
- [4] E. Garrido, J.A. Caballero, E. Moya de Guerra, P. Sarriguren and J.M. Udías, *Nucl. Phys.* **A584** (1995) 256.
- [5] J.A. Caballero, E. Garrido, E. Moya de Guerra, P. Sarriguren, J.M. Udías, *Ann. Phys.* **239** (1995) 351.
- [6] S. Boffi, C. Giusti and F.D. Pacati, *Nucl. Phys* **A476** (1988) 617.

- [7] J.E. Amaro and T.W. Donnelly Ann. Phys. (N.Y.) **263** (1998) 56.
- [8] J.E. Amaro and T.W. Donnelly Nucl. Phys. **A 646** (1999) 187.
- [9] A.S. Raskin and T.W. Donnelly, Ann. Phys. (NY) **191** (1989) 78.